



Commutatorless Motor of Armature-field Perpendicular Type Utilizing D-axis Damper Current

メタデータ	言語: eng 出版者: 公開日: 2010-04-06 キーワード (Ja): キーワード (En): 作成者: Takeda, Yoji, Nishikawa, Shiro, Hirasa, Takao メールアドレス: 所属:
URL	https://doi.org/10.24729/00008573

Commutatorless Motor of Armature-field Perpendicular Type Utilizing D-axis Damper Current

Yoji TAKEDA*, Shiro NISHIKAWA** and Takao HIRASA*

(Received November 15, 1983)

Commutatorless motors are widely used in industries as excellent variable speed motors. They have, however, an important problem that their instantaneous torque contains considerable pulsation. We proposed in a previous paper a commutatorless motor of armature-field perpendicular type which can eliminate this torque pulsation in principle. In this paper we propose a simple method to realize it utilizing d-axis damper current.

1. Introduction

Figure 1 shows the basic construction of the commutatorless motor of armature-field perpendicular type^{1,2)}. In addition to the conventional d-axis field winding, it provides a q-axis field winding. The q-axis field winding is supplied with an alternating current i_q , whose frequency is six times the rotating one. By this means, the resultant field winding axis rotates synchronously with the active armature winding axis, keeping with it the right angle, and the motor will generate a maximum constant torque without pulsation. But this basic construction requires an additional apparatus to generate the sawtooth field current. In this paper a simple method to obtain the sawtooth current by utilizing d-axis damper current is proposed, and the torque pulsation and commutation characteristics are analyzed. Some experimental results are also described.

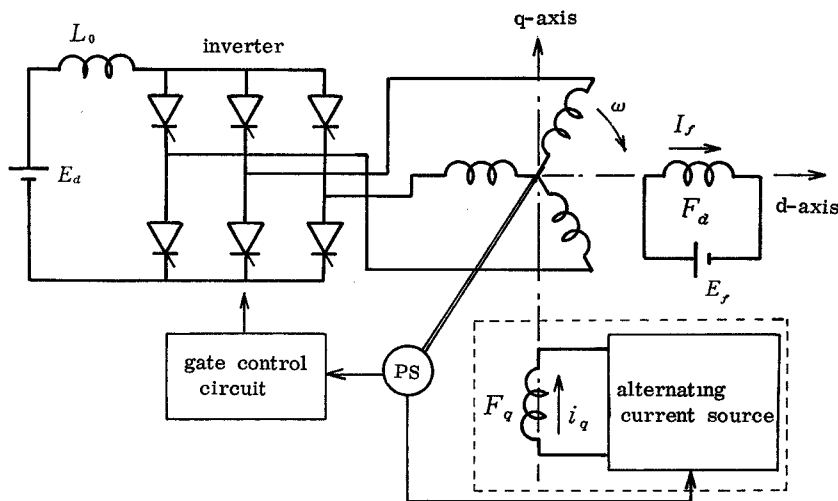


Fig. 1 Basic construction of armature-field perpendicular commutatorless motor.

* Department of Electrical Engineering, College of Engineering.

** Osaka Prefectural Technical College.

2. Basic Principle

Figure 2 shows a basic principle of armature-field perpendicular type commutatorless motor utilizing d-axis damper current. The conventional d-axis field coil acts also as a d-axis damper winding. An alternating current i_{fd} is induced in the d-axis field coil by a periodic fluctuation of equivalent armature winding. The induced current is nearly sawtooth waveform⁹⁾, and this current can be used as a q-axis exciting current. Only the AC component i_{fd} is led to the q-axis field winding through a capacitor C and blocked to flow to the DC source by a reactor L . The frequency of i_{fd} is six times the rotor frequency. Consequently, in the steady state operation, fairly small L and C may well serve for this purpose. In

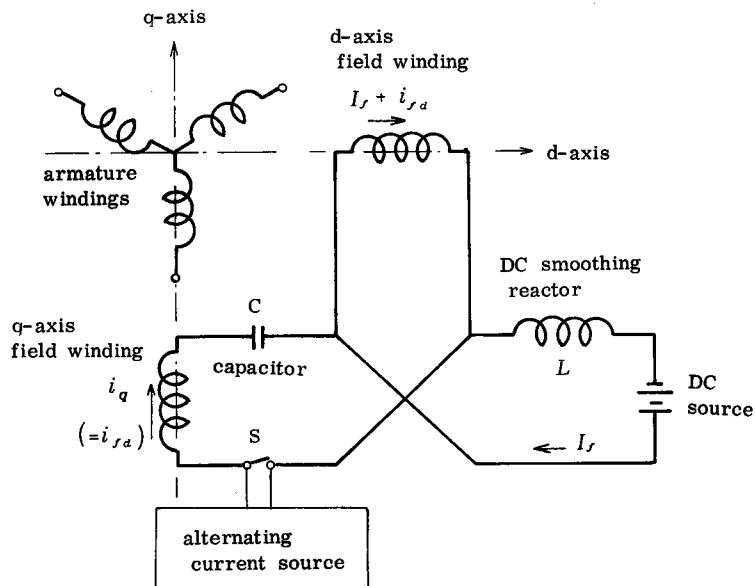


Fig. 2 Basic principle.

this system, the commutation margin angle of advance β must be set to an appropriate value for the stable commutation. If we connect another alternating field current source (dotted part in Fig. 1) with the q-axis winding in series, the d-axis field current is enlarged and a transformer voltage for the commutation is established even if $\beta=0$. As a result, the torque pulsation decreases to a very small value and the motor is able to start by itself.

3. Performance Analysis

3.1 Damper Winding Current

The d-axis field winding shown in Fig. 2 can be separated into two parts as shown in Fig. 3, one conducts AC current and the other conducts DC current. The mutual inductances between the active armature winding and d- or q-field winding are represented by the following equations.

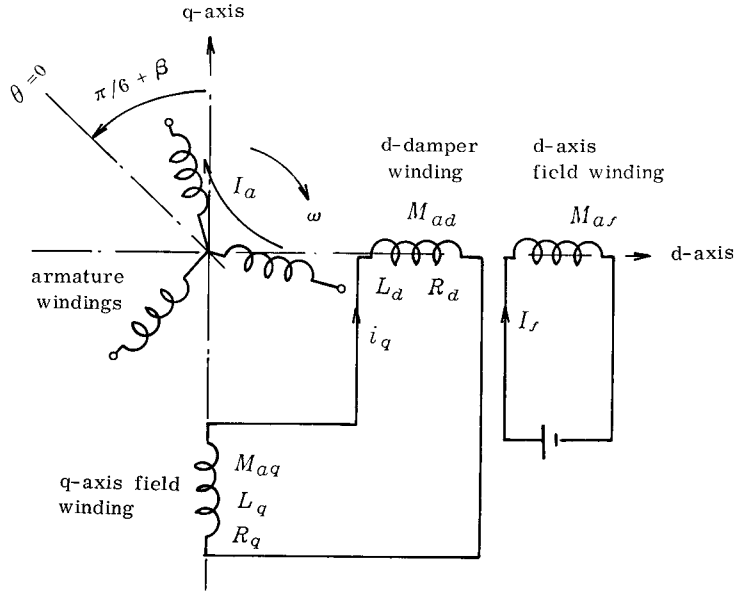


Fig. 3 Equivalent circuit.

$$\mathbf{M}_{af} = M_{af} \sin(\theta - \pi/6 - \beta) = \mathbf{M}_{ad} \quad (1)$$

$$\mathbf{M}_{aq} = M_{aq} \cos(\theta - \pi/6 - \beta) \quad (2)$$

The voltage equation of the damper circuit is

$$p\mathbf{M}_{ad}I_a + (R_d + pL_d)i_q + p\mathbf{M}_{aq}I_a + (R_q + pL_q)i_q = 0 \quad (3)$$

Then,

$$pi_q + \frac{R_{dq}}{L_{dq}} i_q = -\frac{\omega M_{adq}}{L_{dq}} I_a \cos(\theta - \pi/6 + \alpha_M - \beta) \quad (4)$$

where, $p = d/dt$

$$L_{dq} = L_d + L_q, \quad R_{dq} = R_d + R_q$$

$$M_{adq} = \sqrt{M_{ad}^2 + M_{aq}^2}$$

$$\alpha_M = \tan^{-1}(M_{aq}/M_{ad}) = \tan^{-1}n_{qd}$$

$$M_{aq}/M_{ad} = K\sqrt{L_a L_q}/K\sqrt{L_a L_d} = n_q/n_d = n_{qd}$$

n_q : number of turns of q-axis field winding

n_d : number of turns of d-axis field winding

K : coupling coefficient between armature and field windings

If the damper winding resistance R_{dq} is neglected, the solution of Eq. 4 is, (even if R_{dq} is not neglected, the results are almost the same)

$$i_q = \frac{M_{adq}}{L_{dq}} I_a \left\{ \frac{3}{\pi} \sin(\alpha_M - \beta) - \sin\left(\theta - \frac{\pi}{6} + \alpha_M - \beta\right) \right\} \quad (5)$$

Figure 4 shows the calculated results of the normalized current $i_q^N (= i_q L_{dq} / I_a M_{adq})$

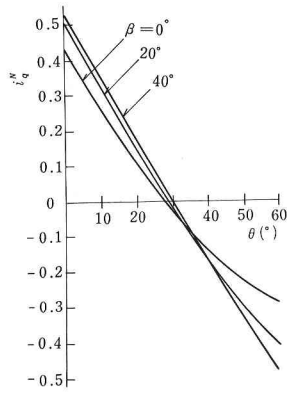


Fig. 4 Damper current ($n_{qd}=1, \alpha_M=\pi/4$).

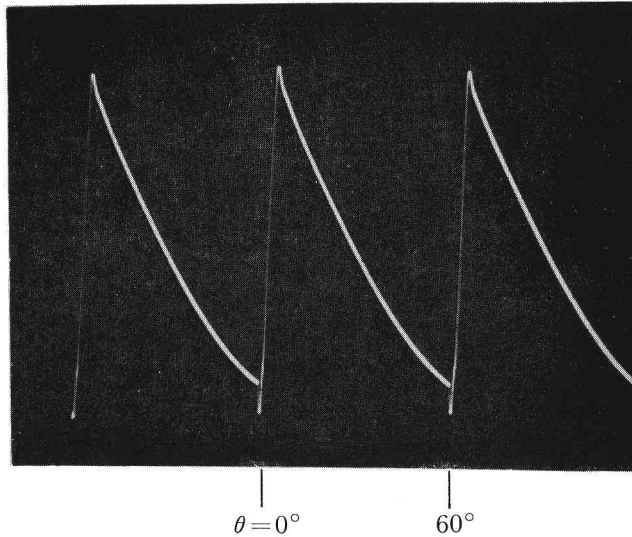


Fig. 5 Experimental damper current ($\beta=20^\circ$).

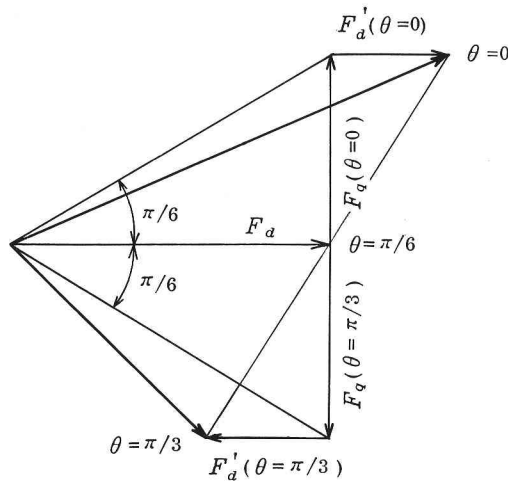


Fig. 6 Resultant MMF of d- and q-axis damper winding.

and Fig. 5 shows the experimental results at $\beta=20^\circ$. Both the figures show, as expected, that q-axis field current is approximately the sawtooth waveform. In this system, as i_q flows through both the d- and q-axis field windings, a d-axis alternating MMF F'_d is generated as well as a q-axis alternating MMF F_q . The resultant MMFs of d- and q-axis field winding are shown in Fig. 6. It is seen that the resultant field MMF has a maximum at $\theta=0$ and a minimum at $\theta=\pi/3$. The displacement from the d-axis is smaller than $\pi/6$ at $\theta=0$ and greater than $\pi/6$ at $\theta=\pi/3$. Consequently, the perfect perpendicular condition of the armature and field is impossible to perform in this system, but nearly perpendicular condition is able to obtain under a certain circumstance.

3.2 Instantaneous Torque

The instantaneous torque for a non-salient machine is given by

$$\tau = I_f I_a \frac{d}{d\theta} M_{af} + i_q I_a \frac{d}{d\theta} (M_{ad} + M_{aq}) \quad (6)$$

The first term of the right side of Eq. (6) represents the essential active torque τ_a , the second term represents the sum τ_{dq} of the torques by the d- and q-axis field windings. From Eqs. (1), (2), (5), and (6)

$$\begin{aligned} \tau = \tau_a + \tau_{dq} = & M_{af} I_f I_a \cos(\theta - \pi/6 - \beta) \\ & + \frac{M_{adq}^2 I_a^2}{L_{dq}} \left[\frac{3}{\pi} \sin(\alpha_M - \beta) \cos\left(\theta - \frac{\pi}{6} + \alpha_M - \beta\right) \right. \\ & \left. - \frac{1}{2} \sin\left\{2\left(\theta - \frac{\pi}{6} + \alpha_M - \beta\right)\right\} \right] \quad (7) \end{aligned}$$

The calculated results of the instantaneous torque at $\beta=20^\circ$ are shown in Fig. 7. τ^N and I_a^N are the normalized values by the following equations.

$$\tau^N = \frac{\tau}{M_{af} I_f I_a}, \quad I_a^N = \frac{L_a I_a}{M_{af} I_f} \quad (8)$$

In this system, by the effect of alternating MMF F'_d , the minimum torque pulsation

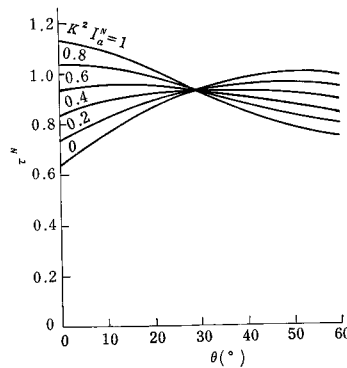


Fig. 7 Instantaneous torque ($\beta=20^\circ$, $n_{qd}=1$).

is not given at $\beta=0$. As i_q is proportional to I_a , in the case of shunt motor, the instantaneous torque is affected by I_a . But in the series motor, the following relationship exists.

$$K^2 I_a^N = \frac{K^2 L_a}{K \sqrt{L_a L_f}} = K \frac{n_a}{n_f} = K n_{af} \tag{9}$$

where

n_{af} : turn ratio of armature winding to d-axis field winding

Therefore, the instantaneous torque of the series motor is not affected by I_a . The torque only depends on the machine structure and β . The calculated results of the torque pulsation ratio R_T at $\beta=20^\circ$ are shown in Fig. 8. R_T becomes fairly small when $K^2 I_a^N$ is about 0.5~0.9 and n_{qd} is about 1~2.5. But, this condition of $K^2 I_a^N$ means a considerable heavy load, so that it is preferable to use a copper machine for this system. One of the methods for reducing the effect of the d-axis alternating MMF is to lead the position of the q-axis field winding by β_q . The calculated results of R_T at $\beta=20^\circ$, $\beta_q=20^\circ$ are shown in Fig. 9. Comparing with Fig. 8, n_{qd} provided with the minimum R_T is smaller than that of $\beta_q=0$.

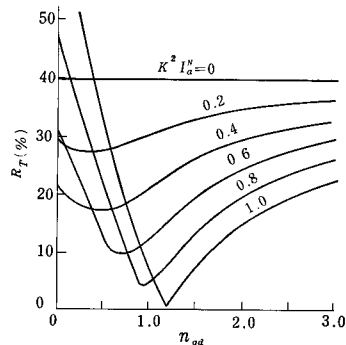
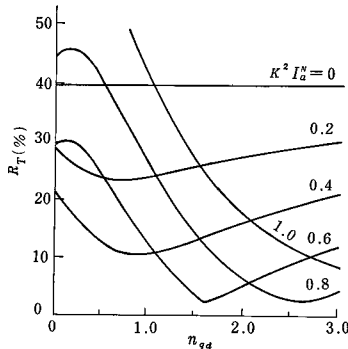


Fig. 8 Torque pulsation ratio ($\beta=20^\circ$).

Fig. 9 Torque pulsation ratio ($\beta=20^\circ$, $\beta_q=20^\circ$).

3.3 Average Torque

The average torque over one commutation period $\pi/3$ is

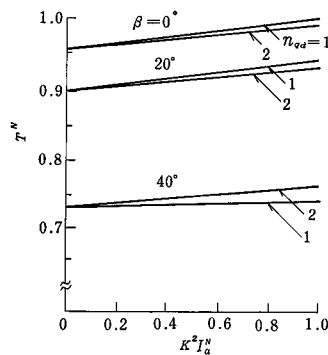


Fig. 10 Average torque.

$$T = 0.955 I_f I_a M_{af} \cos \beta + 0.0425 \frac{M_{adq}^2 I_a^2}{L_{dq}} \sin 2(\alpha_M - \beta) \quad (10)$$

The normalized average torque ($T^N = T / M_{af} I_f I_a$) is shown in Fig. 10. It is seen that the average torque slightly increases with $K^2 I_a^N$ when the condition of small torque pulsation ($\beta = 20^\circ \sim 30^\circ$, $K^2 I_a^N = 0.5 \sim 0.9$, $n_{qd} = 1 \sim 2.5$) is satisfied.

3.4 Instantaneous Induced Voltage of Active Armature Winding

The instantaneous induced voltage of the active armature winding is given as follows.

$$\begin{aligned} e_a &= v_a - R_a I_a \\ &= I_f \frac{d}{dt} M_{af} + i_q \frac{d}{dt} (M_{ad} + M_{aq}) + (M_{ad} + M_{aq}) \frac{d}{dt} i_q \\ &= \omega M_{af} I_f \cos(\theta - \pi/6 - \beta) + \frac{\omega M_{adq}^2 I_a}{L_{dq}} \left[\frac{3}{\pi} \sin(\alpha_M - \beta) \right. \\ &\quad \left. \times \cos(\theta - 6/\pi + \alpha_M - \beta) - \sin\{2(\theta - \pi/6 + \alpha_M - \beta)\} \right] \quad (11) \end{aligned}$$

The normalized induced voltage e_a^N ($= e_a / \omega M_{af} I_f$) at $\beta = 20^\circ$ and $n_{qd} = 1$ is shown in Fig. 11. Though the torque pulsation is minimum when $K^2 I_a^N$ is about 0.5 as shown in Fig. 7. The waveform of e_a^N somewhat declines as indicated in Fig. 11.

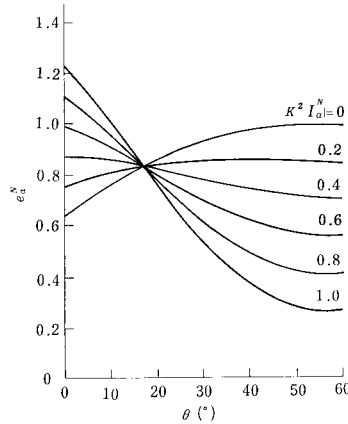


Fig. 11 Instantaneous induced voltage ($\beta = 20^\circ$, $n_{qd} = 1$).

4. Experimental Results

The motor used in the test was a 6 poles, three phase wound type induction motor, rated at 1 KW, 100 V; Its airgap was especially enlarged to 2 mm in order to give it characteristics similar to that of synchronous motor. The two stator windings connected in series are used for d-axis field winding and d-damper winding, and the remaining one for q-axis field winding. Figure 12 shows the q-axis field current and armature terminal voltage of the commutatorless motor of armature-field perpendicular type utilizing d-axis damper current. When i_q

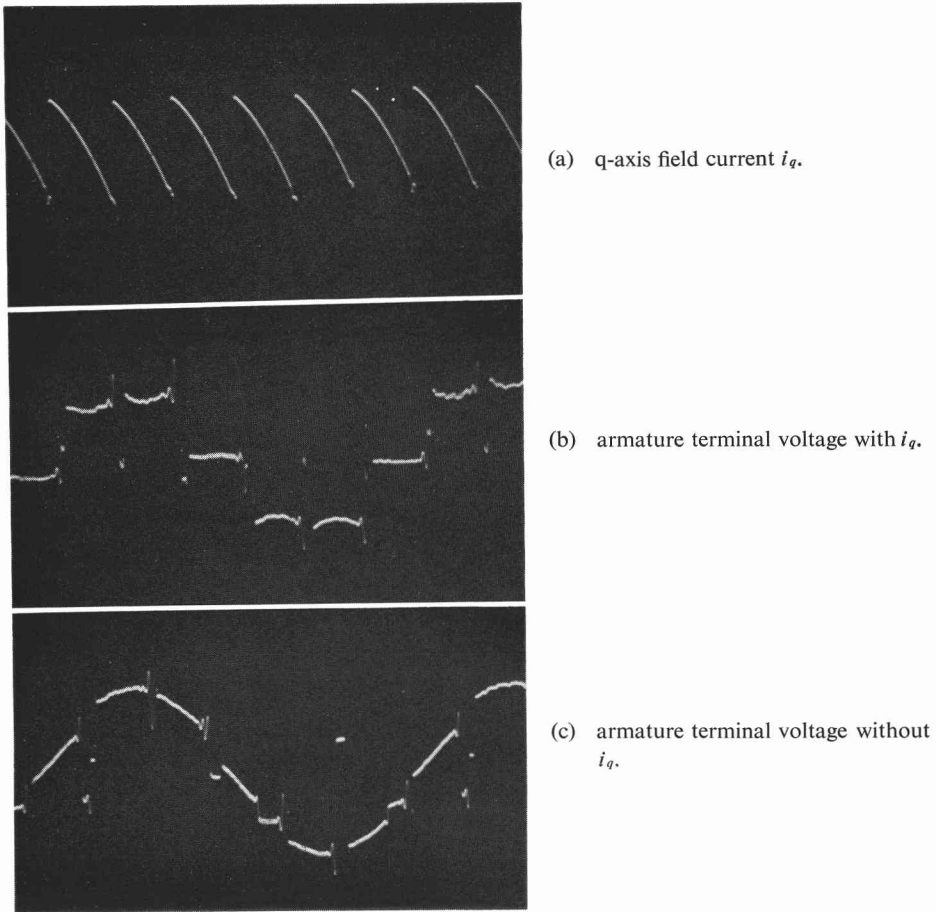
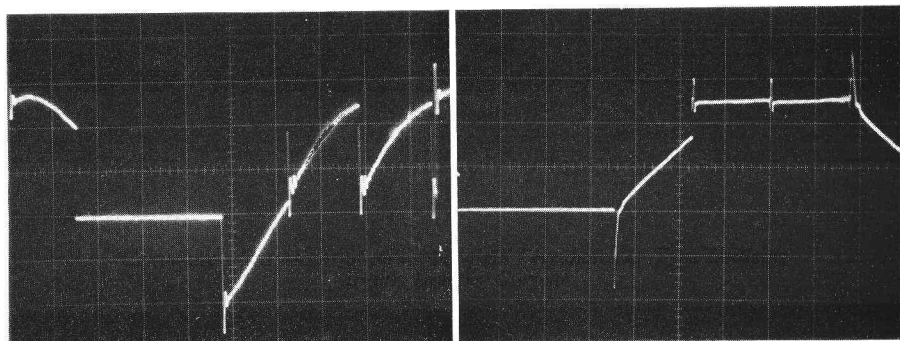


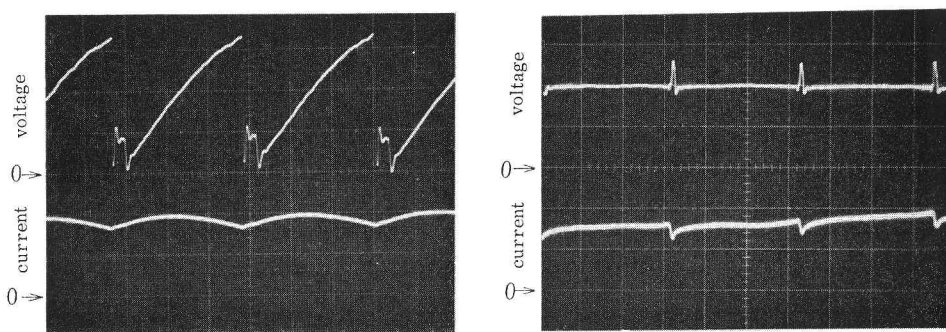
Fig. 12 Experimental waveforms.

conducts, each armature winding of the motor generates a rectangular voltage which is constant throughout the conducting period. It implies that the motor is generating a maximum constant torque without pulsation. The conventional commutatorless motor with load commutation has no commutation voltage at $\beta=0$. Therefore, β must be set to a large value for a stable commutation. Though the system utilizing d-axis damper current has no commutation voltage when $\beta=0$, if the q-axis field current source is inserted to its damper circuit, the motor can be commutated successfully at $\beta=0$ by the transformer voltage from q- and d-axis field windings. The voltage waveform between the anode and cathode of a thyristor in the inverter is shown in Fig. 13. It is observed in Fig. 13 (b) that the inverse voltage is applied upon the thyristor at the end of the commutation period and the thyristor is commutating successfully at $\beta=0$. The terminal voltage and the input current at DC side of the inverter on high speed operation are shown in Fig. 14. Figure 14 (a) shows the waveform in the conventional load commutation system at $\beta=60^\circ$. Though the input current is sufficiently smooth, the terminal voltage varies considerably and the output torque, which is the product of these



(a) conventional commutation type ($\beta = 45^\circ$) (b) type utilizing d-axis damper current ($\beta = 0$)

Fig. 13 Voltage wave forms of thyristor.



(a) conventional commutation type ($\beta = 60^\circ$) (b) type utilizing d-axis damper current ($\beta = 0$)

Fig. 14 Terminal voltage and input current

two values, varies in proportion to the voltage waveform. But in the system utilizing d-axis damper current, the both waveforms of the voltage and current become almost constant as shown in Fig. 14 (b), so that it may be inferred that the torque waveform will contain almost no pulsation.

8. Conclusions

As described above, the system utilizing d-axis damper current has the advantage that it is a very simple method to realize the armature-field perpendicular system. But, because there is the restriction that this system must obtain the q-axis field current from the d-axis damper current, which exerts an undesirable influence upon the performance of this system, the expected results is obtained only when the commutation angle of advance is set about 20° . Accordingly, this system will find it's application in the commutatorless motors with load commutation. The basic system using the q-axis field alternating current source described in the previous paper had the advantage that the torque pulsation becomes zero even at $\beta = 0$ and the motor can start by itself, but it had also the following disadvantages; (1) the q-axis alternating field current source with large capacity is necessary (2) the transformer voltage is excessively high (3) the DC input current is intermitted at every commutation period. If the d-axis damper current is utilized additionally in this basic system, the above advantage is preserved and the disadvantage

is improved as follows; (1) the capacity of the q-axis alternating field current source may be reduced (2) the transformer voltage can be reduced to an acceptable value (3) the DC input current doesn't intermitted.

References

- 1) T. Hirasu, Y. Takeda and S. Nishikawa, Society on SPC of IEEJ, SPC-81-12 (1981)
- 2) Y. Takeda, S. Nishikawa and T. Hirasu, Bull. Univ. of Osaka Prefecture, A.32, 9 (1983)
- 3) Y. Takeda, S. Yasuoka and T. Hirasu, Trans. IEEJ, 96-B, 123 (1976)